Journal of Applied Polymer Science

A commercial production route to prepare polymer-based nanocomposites by unmodified multilayer graphene

Xubing Fu,[1] Yan Liu,[2] Xingke Zhao,[3] Dajiang Zhao,[1] Guisheng Yang[1,2,3]

[1]School of Chemistry and Chemical Engineering, Hefei University of Technology, Hefei, Anhui 23009, China
[2]Shanghai Genius Advanced Material Co., Ltd, Shanghai 201109, China
[3]Department of Polymer Science and Engineering, Zhejiang University, Hangzhou, Zhejiang 310027, China
Correspondence to: G. Yang (E-mail: ygs1211@sina.com)

ABSTRACT: In this study, we report our progress toward an effective method to prepare polyamide 6 (PA6)/multilayer graphene (MLG) nanocomposites via *in situ* polymerization. The thermal and mechanical properties of PA6 nanocomposites were investigated with low unmodified MLG content of 0.01–0.5 wt %. The dispersion of MLG sheets in the host matrix was studied in extensive detail while the properties of the resultant nanocomposites were systematically measured. Results indicate that the mechanical properties of the nanocomposites were significantly enhanced; the flexural modulus, flexural strength and impact strength increased by ~97%, ~69%, and ~76% relative to pristine PA6. Furthermore, the thermal stability of nanocomposites was enhanced and the weight loss temperature of PA6 was increased ~15°C at 0.5 wt % content of MLG. Moreover, incorporation of low loading of MLG can increase the crystallization speed of PA6 composites and promote the formation of the γ-crystalline phase while also improving the crystallization temperature. © 2015 Wiley Periodicals, Inc. J. Appl. Polym. Sci. **2015**, *132*, 42742.

KEYWORDS: graphene and fullerenes; mechanical properties; nanostructured polymers; nanotubes; polyamides; synthesis and processing

Received 5 May 2015; accepted 14 July 2015
DOI: 10.1002/app.42742

INTRODUCTION

Graphene is the first two-dimensional (2D) atomic crystal available for synthesis and application.[1] It can be stacked into 3D graphite, rolled into 1D nanotubes, or wrapped into 0D fullerences.[2] As a nanocarbon material, it has attracted great attention due to its superior electronic, thermal and mechanical properties.[3–6] These intrinsic properties of graphene have generated enormous interest for its possible incorporation in polymer/graphene nanocomposites.[7] Therefore, the investigation of polymer/graphene nanocomposites has been extensively conducted in recent years, in which various forms of graphene and its derivatives/polymer composites have been widely produced including polycarbonate, polyethylene, epoxy, poly(methyl methacrylate), polypropylene and so on.[8–17] Therefore, the discovery of graphene, with its combination of extraordinary physical properties and its ability to be dispersed in various polymer matrices, has created a burgeoning class of polymer composites.

PA6 is an important thermoplastic with a wide range of engineering applications. It has many advantageous properties that include abrasion resistance, oil resistance, chemical resistance, good elasticity, and it can be self-extinguished. However, its mechanical performance, such as strength and modulus, is insufficient and limits its application.[7] Therefore, many works have focused on the improvement of its mechanical properties through the introduction of nanofillers.[18,19] PA6 composites reinforced with graphene have attracted much attention because of recent publications that report substantial improvements in the mechanical and other various physical properties.[3,7,20,21] However, the hydrophobic and nonpolar nature in graphene causes poor dispersion in a variety of polymer matrices, while the intrinsic van der Waals forces and high surface area promote re-aggregation and re-stacking.[22–24] Due to this phenomenon, the interaction between pure graphene (unmodified graphene) sheets and PA6 matrix is considered to be unfavorable; therefore, chemical modification (such as functionalization) is needed to achieve a good dispersion and strong interface interaction of graphene in polymer composites.[21,25–28] Accordingly, modified graphene has more reactive groups than unmodified graphene, which makes it easier to form a fine dispersion and strong hydrogen bonds in the polymer matrix. Several chemical modification methods have been used to improve the dispersion and compatibility of graphene with the PA6 matrix. For example, Xu[21] reported an efficient method through chemical reduction of graphene oxide (GO) to prepare PA6/graphene composites by *in situ* polymerization. During polycondensation,

Table I. Ultrasonic Data of PMLG Samples with 0.05 wt % Content of MLG (Ultrasonic in a Beaker of 1000 mL and the Volume of Solution is 800 mL)

Samples	MLG loading (wt %)	Ultrasonic power (w)	Total ultrasonic time (min)	Samples	Ultrasonic power (w)	Total ultrasonic time (min)
1	0.05	250	5	8	100	20
2	0.05	250	10	9	150	20
3	0.05	250	15	10	200	20
4	0.05	250	20	11	250	20
5	0.05	250	30	12	300	20
6	0.05	250	40	13	400	20
7	0.05	250	50	14	500	20

GO was thermally reduced to graphene, simultaneously, and they found that the tensile strength, and Young's modulus of composite fibers clearly increased with a mere GO loading of 0.1 wt %. Zhang *et al.*[3] demonstrated an efficient approach to prepare PA6/GO nanocomposites via *in situ* polymerization, in which GO was directly used. The results showed that the tensile strength and Young's modulus of the composites were substantially improved with low content of GO. Liu *et al.* prepared the PA6/functionalized graphene (FG) nanocomposites fibers by a method that functionalizes GO. PA6 chains were successfully grafted from FG sheets. It was found that incorporation of polymer-grafted graphene can enhance the mechanical properties of fibers and the tensile strength can be improved by 29% with a graphene loading of 0.1 wt %. Though it is rather more compatible with polymers than the pure graphene, the properties (i.e., mechanical properties) of the modified graphene is more obviously altered due to the chemical modification process compared with those of the pure graphene.[29–31] In addition, the modification process is time-consuming and creates undesired pollutants; therefore, using the unmodified graphene to reinforce the polymers may be more effective and more suitable for commercial production relative to the modified material. This research is also driven by the lack of publications investigating the unmodified graphene influence on polymer properties.

Herein, we report our progress toward an effective method to prepare PA6-unmodified graphene nanocomposites via *in situ* polymerization. As a fact, it is very difficult to obtain the 100% single-layer graphene (SLG) on a large scale for commercial production. The graphene used in this work is multilayer graphene (MLG) and is expected to be used as an economical material for large-scale production of various advanced graphene-based products. Under the assistance of an ultrasonic cell crusher at optimal ultrasonic power and time, the MLG sheets can be well dispersed in melted ε-caprolactam. The thermal and mechanical properties of PA6/MLG (PMLG) nanocomposites with different contents of MLG were investigated. It is found that the strength and modulus of PMLG composites were dramatically increased with only minimal amounts of MLG loading. Moreover, the process for the preparation of PMLG nanocomposites is more cost-effective, creates less pollution, quicker and more suitable for large-scale industrial production relative to PA6-modified graphene nanocomposites.

EXPERIMENTAL

Materials

Commercial multilayer graphene powder was supplied by Hefei Weijing Materials. Commercial grade ε-caprolactam (CL, purity ≥ 99%) was obtained from Nanjing Oriental Chemical. Semiconductor grade-Sodium hydroxide (NaOH, 99.99% metal basis) was purchased from Sinopharm Chemical Reagent. Toluene-2, 4-diisocyanate (TDI, HPLC 99.5%) was purchased from Shanghai Chemical Reagents.

Preparation of PA6/Multilayer Graphene Nanocomposites

A typical procedure to prepare PMLG nanocomposites was depicted as follows: a desired amount of MLG powder was added to molten ε-caprolactam, the mixture was sonicated by an ultrasonic cell crusher (JY92-IIDN, 20–25KHZ, 900W, Ningbo Scientz, China). Then, the mixture was quickly transferred into a three-necked round-bottom flask and sodium hydroxide (5 wt %) as a catalyst for anionic ring opening polymerization was added, which was kept under a vacuum at 180°C for 30 min to remove the water. Subsequently, 0.5 wt % toluence-2, 4-diisocyanate (TDI) (used as an activator) was added with stirring, the final mixture was quickly poured into a mold preheated to 160°C, and polymerized in the oven at 160°C for 15 min. The products were slowly cooled to room temperature and purified with boiling water to eliminate the residual monomer or low molecular weight oligomer.

As the ultrasonic power and time are the two main factors that influence the result of the dispersion, many experiments were performed varying these parameters in order to find the optimal settings. For example, seven samples with 0.05 wt % content of MLG were sonicated for 5, 10, 15, 20, 30, 40, and 50 min with the same ultrasonic power of 250 W. According to the above steps, seven PMLG nanocomposites were prepared and named as samples 1–7, respectively. After we compared the dispersion of each of the samples, the optimal total ultrasonic time was found to be about 20 min. Then, another set of seven samples with 0.05 wt % content of MLG were sonicated for 20 min with different power settings of 100, 150, 200, 250, 300, 400, and 500 W and were named samples 8–14, respectively. The dispersion of samples 8–14 was evaluated and the optimal ultrasonic power was found to be 250 W for 0.05 wt % content. According to this experiment process, other samples with different content of MLG were also observed. Table I lists the samples with different ultrasonic time and power of the experiments

Table II. Optimal Ultrasonic Data of PMLG Samples (Ultrasonic in a Beaker of 1000 mL and the Volume of Solution is 800 mL)

MLG loading (wt %)	Optimal ultrasonic power (w)	Optimal total ultrasonic time (min)
0.01	~200	~15
0.05	~250	~20
0.1	~250	~25
0.5	~300	~25

(0.05 wt %). Table II lists the optimal ultrasonic time and power of samples with different content of MLG in this work.

In the end, the PMLG nanocomposites (Figure 1) with different amounts of MLG (0.01, 0.05, 0.1, and 0.5 wt %) were obtained (the samples were all sonicated with the optimal ultrasonic power and time). They were noted as PMLG 0.01, PMLG 0.05, PMLG 0.1, and PMLG 0.5, respectively.

Characterization and Instruments

Raman spectroscopy measurements were obtained using a SPEX-1403 laser Raman spectrometer with excitation provided in back-scattering geometry by a 514 nm argon laser line.

High-resolution transmission electron microscopy (HR-TEM) was conducted using a 200 kV F20ST (FEI Company). Transmission electronic microscopy (TEM) was carried out on a Hitachi H-800 microscope at an acceleration voltage of 100 kV. The samples were ultra microtomed with a diamond knife on a Leica Ultracut UCT microtome at −20°C to give 70 nm thick sections.

Field emission scanning electron microscopy (FE-SEM) images were taken on a Hitachi S4800 field-emission SEM system.

X-ray photoelectron spectroscopy (XPS) measurements were performed in a VG ESCALB MK-II electron spectrometer, using a monochromatic Al Kα X-ray source operated at 1486 eV.

A waters-991 gel permeation chromatography (GPC) instrument was used to evaluate the weight-average molecular weight ($\bar{M}_w$), the number-average molecular weight ($\bar{M}_n$) and the polydispersities ($\bar{M}_w/\bar{M}_n$) of the PA6 nanocomposites. All of the samples were solved by *m*-cresol and MLG was filtered off.

Thermal gravimetric analysis (TGA) was performed using a SDT Q600 (USA TA Instrument Corporation) at a heating rate of 20°C/min from 50 to 600°C in a nitrogen atmosphere.

The melting and crystallization behaviors of PMLG nanocomposites were characterized using a NETZSCH DSC 200PC

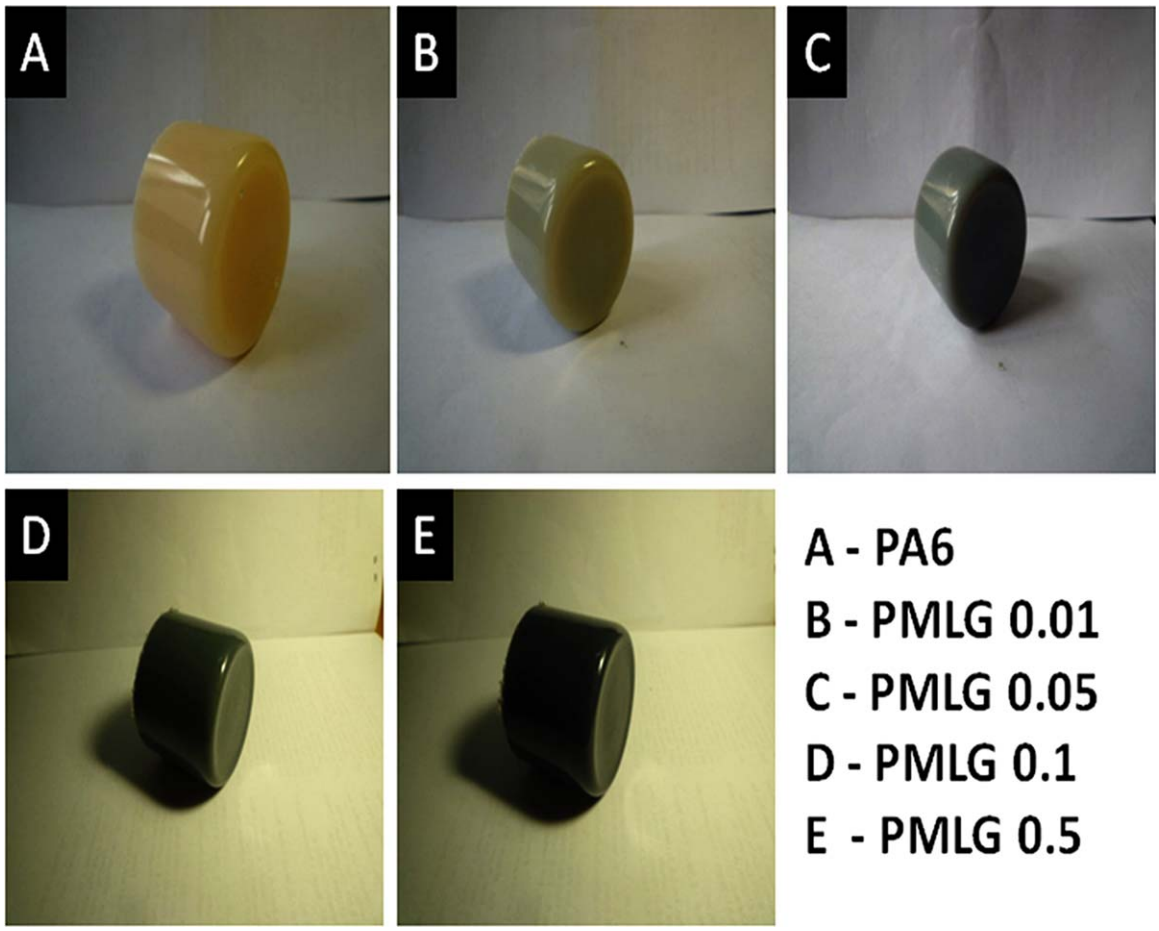

Figure 1. The PMLG samples with different content of MLG: A–E is 0, 0.01, 0.05, 0.1, and 0.5 wt %, respectively. [Color figure can be viewed in the online issue, which is available at wileyonlinelibrary.com.]

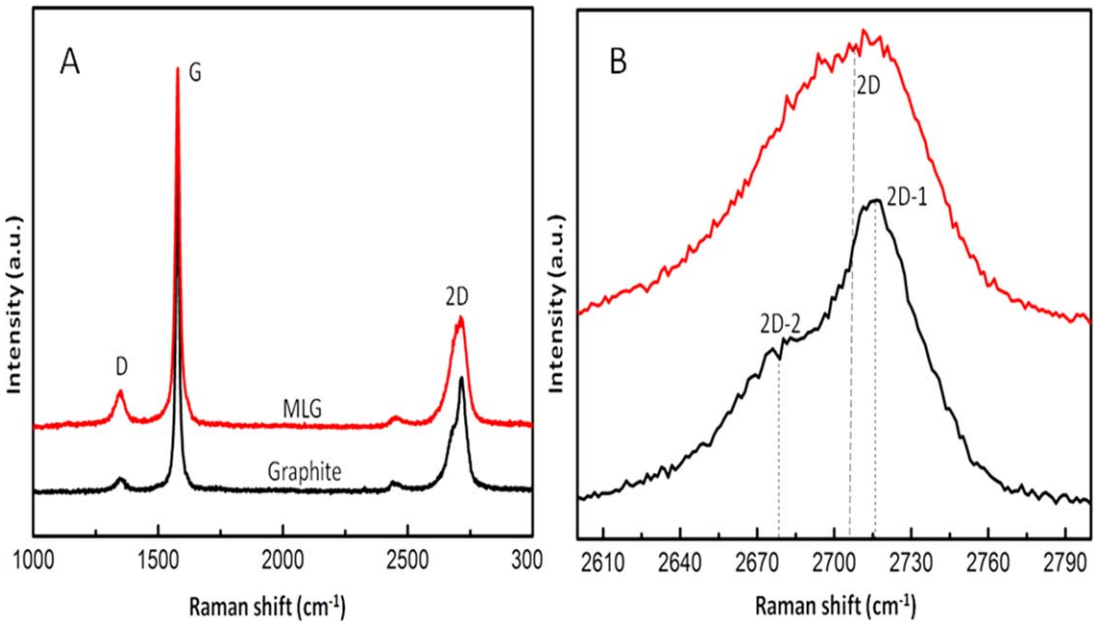

Figure 2. Raman spectra of (A) graphite and multilayer graphene samples, (B) the enlarge image of 2D peaks. [Color figure can be viewed in the online issue, which is available at wileyonlinelibrary.com.]

differential scanning calorimeter (DSC). The pristine PA6 and PMLG were first heated from 50 to 260°C at a heating rate of 10°C/min under a nitrogen atmosphere and kept for 5 min to erase the thermal history. The crystallization behaviors were recorded from 260 to 50°C at cooling rates of 10°C/min. Then the samples were second heated from 50 to 260°C at a heating

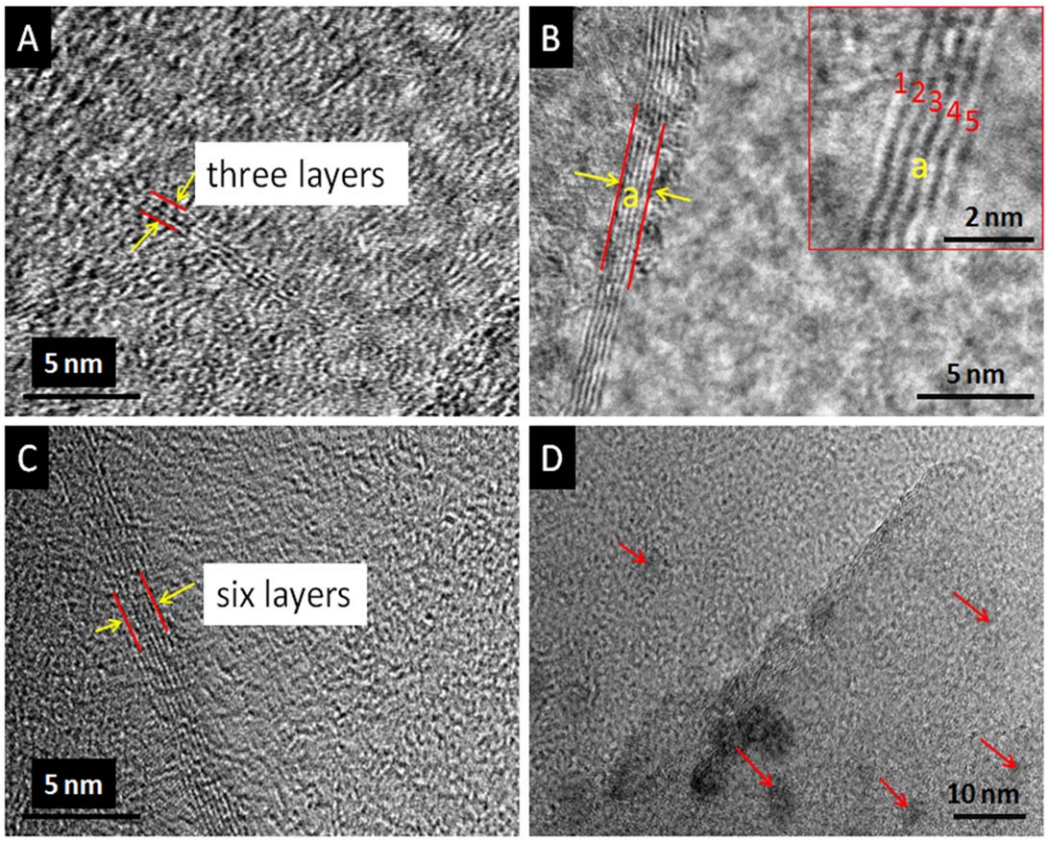

Figure 3. The HR-TEM images of multilayer graphene powder: (A) three layers of graphene sheets; (B) five layers of graphene sheets; (C) six layers of graphene sheets; (D) three to dozens of graphene sheets. [Color figure can be viewed in the online issue, which is available at wileyonlinelibrary.com.]

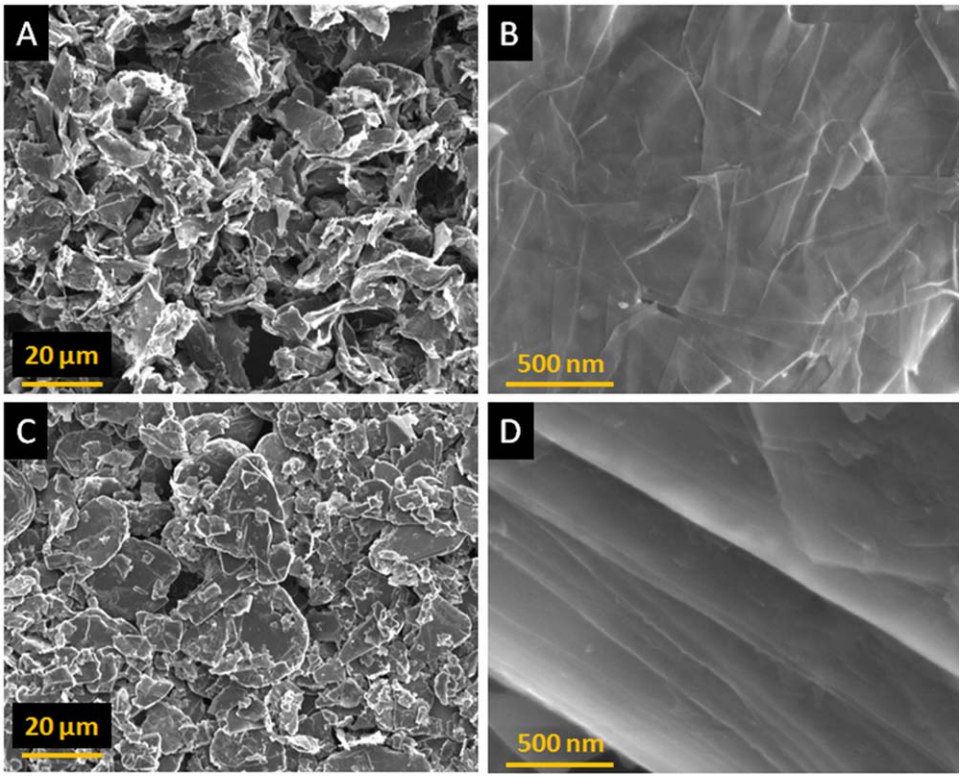

Figure 4. The FE-SEM images of graphite and multilayer graphene powder: (A) and (B) are the images of graphite powder; (C) and (D) are the images of multilayer graphene powder. [Color figure can be viewed in the online issue, which is available at wileyonlinelibrary.com.]

rate of 10°C/min. The melting temperature (T_m) and the degree of crystalline (X_c) were determined from the heating scan.

The tensile test of PA6 and PMLG were performed by using an Instron 1122 machine at room temperature, according to ASTM D 638 standard at a crosshead speed of 50 mm/min. The IZOD notched impact strength was measured according to ASTM D 256, using an IZOD machine Model CSI-137D. The flexural strength and Young's modulus were measured according to ASTM D 790.

RESULTS AND DISCUSSION

Analysis of the Raw Multilayer Graphene

Raman spectroscopy is considered to be an effective tool to characterize the layers of graphene. There are three apparent peaks in the Raman spectra lines of graphene and graphite from 1000 to 3000 cm^{-1}: the D peak (~1350 cm^{-1}) refers to the disordered fractions, G peak (~1580 cm^{-1}) refers to the graphitic ordering, and 2D peak (~2700 cm^{-1}) confirms the presence of the graphene layers.[32] The obvious difference between the spectra is the intensity shape and position of the 2D band.[33] Figure 2(A) shows the Raman spectra of graphite powder and MLG powder. The G line (~1583 cm^{-1}) and 2D line (~2700 cm^{-1}) are visible in the two samples. Figure 2(B) clearly shows the Raman 2D bands; there are two apparent peaks in the 2D band of graphite powder (2D-1 and 2D-2), while there is only one main peak in the 2D band of MLG. MLG powder shows a shift in the 2D band that is attributed to thinner flake graphene material. The graphene layers are estimated to be between several to dozens of layers.[34] HR-TEM is implemented to measure the layers of the material. Figure 3 shows the typical HR-TEM images of MLG in which the number of MLG layers is about 3–25 at a total thickness of 1–9 nm.

Figure 4 illustrates the FE-SEM images of graphite and MLG powder. It can be seen clearly that the images of graphite are different from that of MLG, the graphite sheets appear

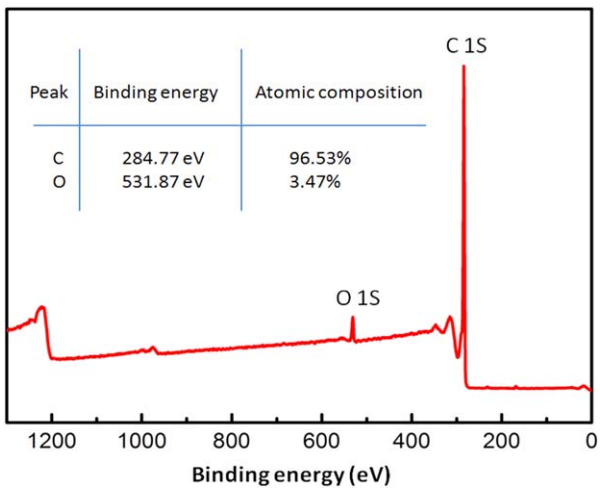

Figure 5. Wide-scan XPS spectra of multilayer graphene. [Color figure can be viewed in the online issue, which is available at wileyonlinelibrary.com.]

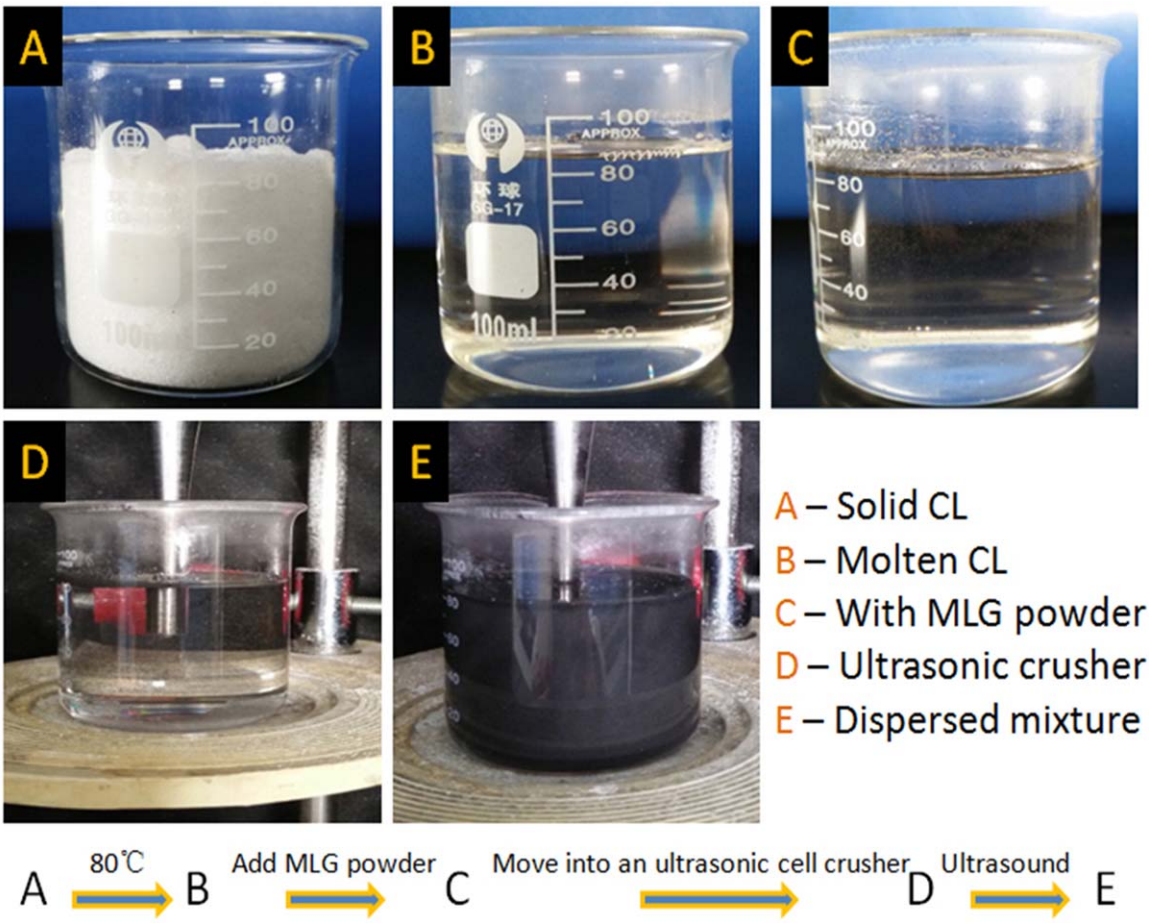

Figure 6. A schematic for the process of dispersion (the multilayer graphene dispersed in molten ε-caprolactam). [Color figure can be viewed in the online issue, which is available at wileyonlinelibrary.com.]

agglomerated and wrinkled, while the MLG sheets are flat and stratified.

XPS was used to determine the elemental composition and binding energy of graphene.[35] The XPS spectrum of MLG powder (Figure 5) showed that the sample consisted of 3.47% oxygen and 96.53% carbon.

Multilayer Graphene Dispersion in Molten ε-Caprolactam

In order to improve the dispersibility of nanofillers in polymers, conventional measures such as mechanical stirring, magnetic stirring, and ordinary ultrasonication, were implemented in previous works. As these measures require long durations of time (several to tens of hours) and result in high costs, it is imperative to devise an alternative method that can reduce the time of processing.[36] Thus, an approach to achieve a good dispersion of MLG in polymer matrix with a simple, time-saving, and low-cost process was devised in this work. The approach used to disperse MLG in molten CL by the ultrasonic cell crusher is discussed in detail in section "Preparation of PA6/Multilayer Graphene Nanocomposites". Figure 6 displays the simple schematic process of MLG dispersion and the results are shown in Figure 7.

As seen in Figure 7, the sample in Figure 6(A) appears to be almost entirely filled with the MLG sheets, while the MLG sheets of typical stretched or wrinkled pattern are randomly dispersed in PA6 regions. The relatively white regions are attributed to the MLG sheets compared to the gray regions of the matrix. It showed much more uniformly dispersed regions without large agglomeration, implying that the MLG sheets were well-dispersed in the PA6 matrix. Figure 6(B) illustrates that MLG sheets are tightly embedded within the polymer (the red arrow represents MLG sheets and the blue arrow represents the area of PA6 matrix), indicating that the interfacial interaction between MLG sheets and PA6 matrix are well-adhered. Figure 6(C) shows the morphology of the tensile fracture surface of the PMLG samples, in which the tough surface upon fracture can be attributed to the strong interfacial adhesion and good compatibility between MLG and PA6 matrix.[37–39] It is difficult to explain the forces amongst MLG sheets and PA6 matrix, it may be due to the nano-effect or the intercalation effect, but requires a more in depth study. Figure 6(D) shows the TEM images of samples, displaying good dispersion of MLG sheets on the macro scale, but has a slight tendency to agglomerate in the nanosheets. The small aggregation of nanosheets may be attributed to the strong van der Waals interactions between the nanolayers.[40] HR-TEM was used to evaluate the morphology of the MLG sheets after ultrasonication. Figure 3(B) shows the HR-TEM image of MLG sheets. As

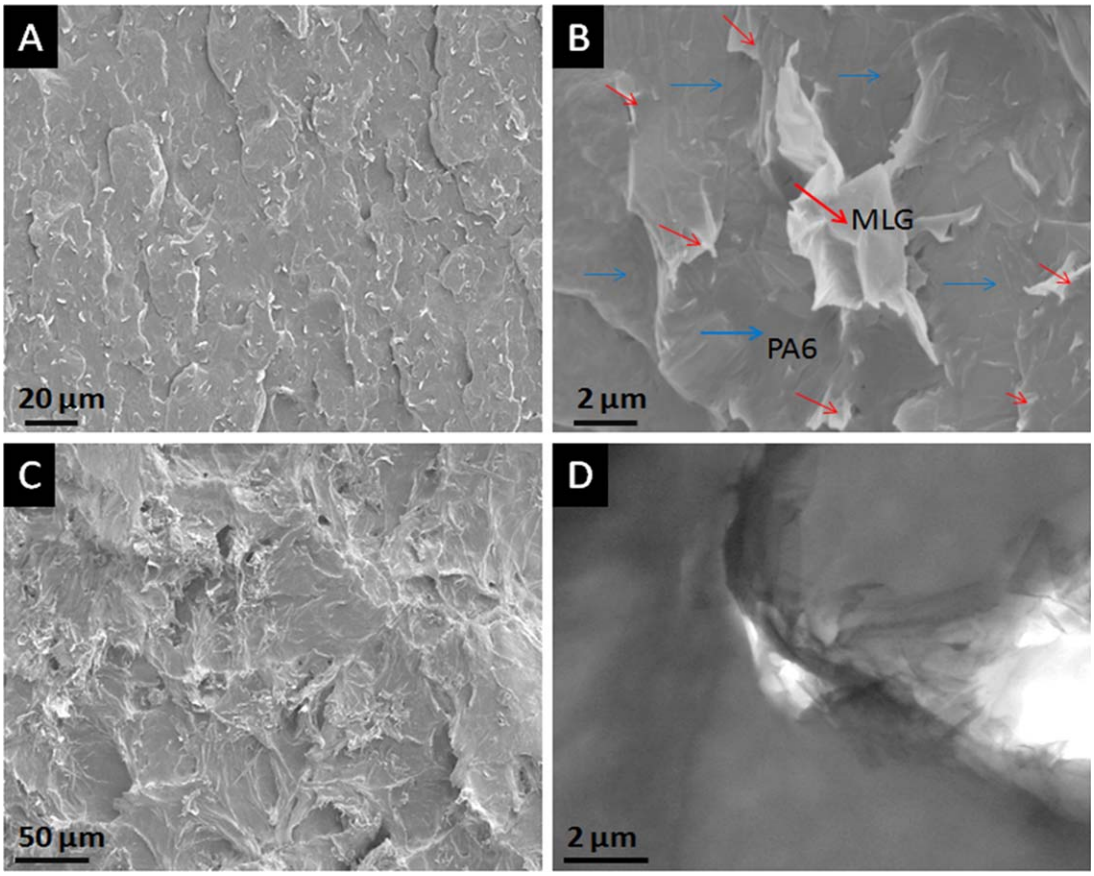

Figure 7. The FE-SEM and TEM images of PA6/MLG samples containing 0.05 wt % MLG: (A), (B), and (C) are the FE-SEM images; (D) is the TEM image. [Color figure can be viewed in the online issue, which is available at wileyonlinelibrary.com.]

shown by the yellow arrows and red lines, the parallel dark lines of layers are clearly apparent, which indicates that the MLG sheets are not destroyed by ultrasonication.[41,42]

Molecule Weight

Table III lists the $\bar{M}_w$, $\bar{M}_n$, and $\bar{M}_w/\bar{M}_n$ of PA6 nanocomposites. It can be seen that the $\bar{M}_w$ and $\bar{M}_n$ of PA6 nanocomposites shows a small decrease as the content of MLG increases, indicative of the MLG additions having no obvious effect on the molecule weight of PA6 nanocomposites.

Thermal Stability

Thermal stability is an important property for PA-based composites as they are potentially used as high-performance engineering plastics.[37] TGA was carried out under a nitrogen atmosphere and performed on all PMLG samples with different contents of MLG. The resulting curves are shown in Figure 8.

In the case of pristine PA6, the 5% weight loss below 390°C was attributed to the decomposition of the lower molecular weight polymer, the main weight loss between 390 and 500°C was

Table III. Molecule Weight Data of PA6 and PMLG Samples

Samples	$\bar{M}_w$ (kg/mol)	$\bar{M}_n$ (kg/mol)	$\bar{M}_w/\bar{M}_n$
PA6	~51.3	~22.1	2.32
PMLG 0.01	~50.7	~21.6	2.35
PMLG 0.05	~49.8	~21.2	2.35
PMLG 0.1	~49.2	~20.5	2.40
PMLG 0.5	~46.3	~19.4	2.39

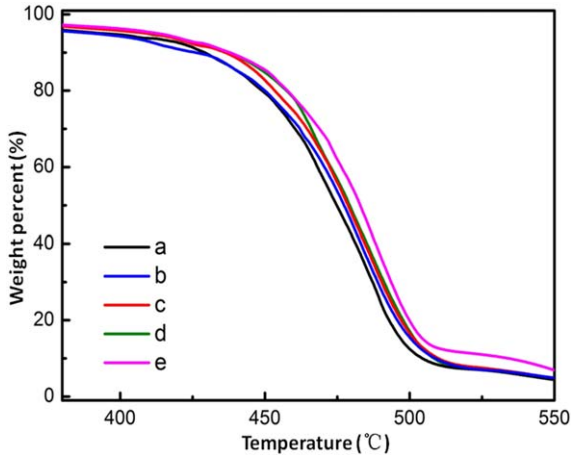

Figure 8. The TGA curves of pristine PA6 and PMLG nanocomposites: (a) PA6; (b) PMLG 0.01; (c) PMLG 0.05; (d) PMLG 0.1, and (e) PMLG 0.5. [Color figure can be viewed in the online issue, which is available at wileyonlinelibrary.com.]

Table IV. TGA Data of PA6 and PMLG Samples

Samples	$T_{5\ wt\ \%}$ (°C)	T_{max} (°C)	$T_{95\ wt\ \%}$ (°C)	Residue at 550°C (wt %)
PA6	394.2	449.36	544.5	4.41
PMLG 0.01	390.7	451.67	548.7	4.46
PMLG 0.05	409.0	452.41	545.9	4.73
PMLG 0.1	409.4	453.75	548.0	4.89
PMLG 0.5	412.4	457.40	559.2	6.89

attributed to the decomposition of higher molecular weight polymer.[22] In the case of PMLG samples, the 5% weight loss temperature increases from ~390 to ~410°C with increasing MLG content with the main mass loss occurring at around 390–530°C, which is higher than that of pristine PA6. Moreover, the maximum weight loss temperature (T_{max}) also increases from 449°C (pristine PA6) to 457°C (PMLG 0.5) and the 95% weight loss temperatures are increased by 1–15°C (Table IV). These indicate that the thermal stability of PA6 was improved by incorporation of MLG. It is in accordance with the report that upon the addition of nanofillers, especially graphene to the polymers, these nanofillers can penetrate into the complex structures in order to modify the structure of the polymer such that thermal stability of the composite will be improved.[43,44] In addition, the residues at 550°C are not relatively increased, which might be because of the amount of MLG was too low to influence the final residues of the composites.[45]

Crystallization Characteristics

DSC is an important tool to determine the melting and recrystallization behavior in the materials.[10,46] A typical nonisothermal crystallization and melting behavior of PA6 and PMLG nanocomposites were studied by DSC. Figure 9 displays the second heating DSC curves and cooling curves of PA6 and PMLG samples with different MLG contents, the data is summarized in Table V in detail. Figure 9(A) shows the second heating curves, pristine PA6 displays only one melting peak at about 223°C, while PMLG samples show two distinct melting peaks, one main peak at about 222°C ~217°C (T_{m1}) and other peak at about 213–210°C (T_{m2}), indicating the coexistence of α and γ crystalline form of PMLG nanocomposites or the process related melting–recrystallization during the second heating scan.[47] As the MLG contents increases, the relative intensity of the peak about T_{m1} (α-crystalline) decreases, whereas the peak about T_{m2} (γ-crystalline) increases, at 0.5 wt % the intensity of the two peaks (217 and 210°C) is similar, which is more evidence that nanoscale dispersed MLG promotes the formation of the γ-crystalline.[48] The melting peak of T_{m1} at 223°C moves to lower temperatures with MLG content increasing and the peak of T_{m2} at 213°C also moves to a lower temperature. Moreover, the peak of α-crystalline becomes weaker and broader with the increase of MLG loading, implying the incomplete α-crystalline for the restricted mobility of polymer chains, which is a significant dynamic factor to form crystals by arrangements of polymer chains.[21]

The cooling curves of PA6 and PMLG samples are shown in Figure 9(B). As seen in Figure 9(B) and Table V, the PMLG samples have higher crystallization temperatures (T_c) than that of the pristine PA6 at all cooling rates. The T_c increased from ~171.2°C of pristine PA6 to ~185.1°C of 0.5 wt % PMLG sample. This significant increase of T_c is attributed to the

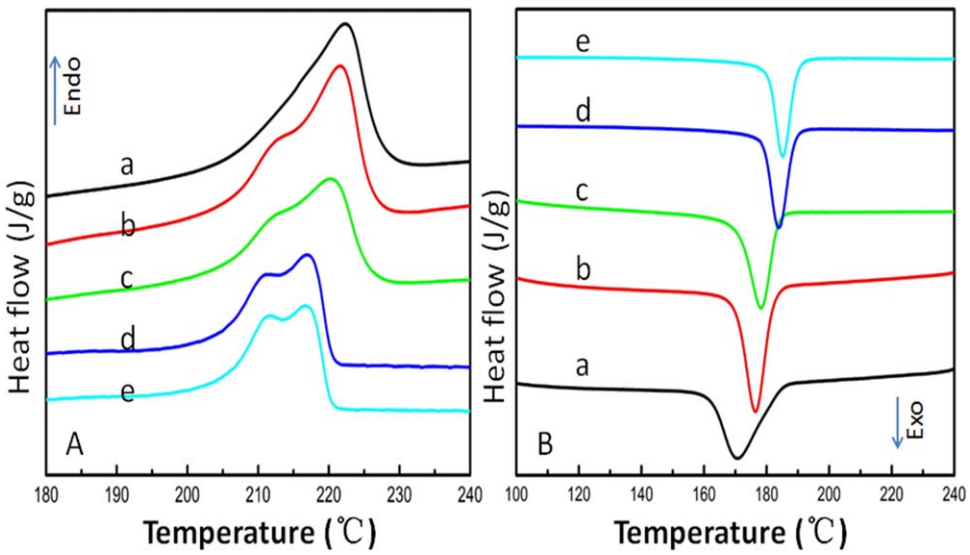

Figure 9. The DSC second heating scans (A) and cooling scans (B) of pristine PA6 and PMLG nanocomposites: (a) PA6; (b) PMLG 0.01; (c) PMLG 0.05; (d) PMLG 0.1, and (e) PMLG 0.5. [Color figure can be viewed in the online issue, which is available at wileyonlinelibrary.com.]

Table V. DSC Average Data of Melt Crystallization for PA6 and PMLG Samples

Samples	T_{m1} (°C)	T_{m2} (°C)	ΔH_m (J/g)	X_c (%)	T_c (°C)
PA6	~223		~60.5	~31.8	~171.2
PMLG 0.01	~222	~213	~63.1	~33.2	~175.9
PMLG 0.05	~220	~212	~63.9	~33.6	~177.4
PMLG 0.1	~217	~210	~66.1	~34.8	~183.9
PMLG 0.5	~217	~210	~62.4	~32.8	~185.1

heterogeneous nucleation induced by the 2D MLG nanosheets during crystallization of PA6.[10] The data about the degree of crystallinity (X_c) is also listed ($X_c = \Delta H/\Delta H_{100}F$, where$\Delta H$ is the enthalpy of fusion, ΔH_{100} is the enthalpy of fusion for a 100% crystalline PA6 which was taken to be 190 J g^{-1}, the factor F denotes the fraction of polymer present in the

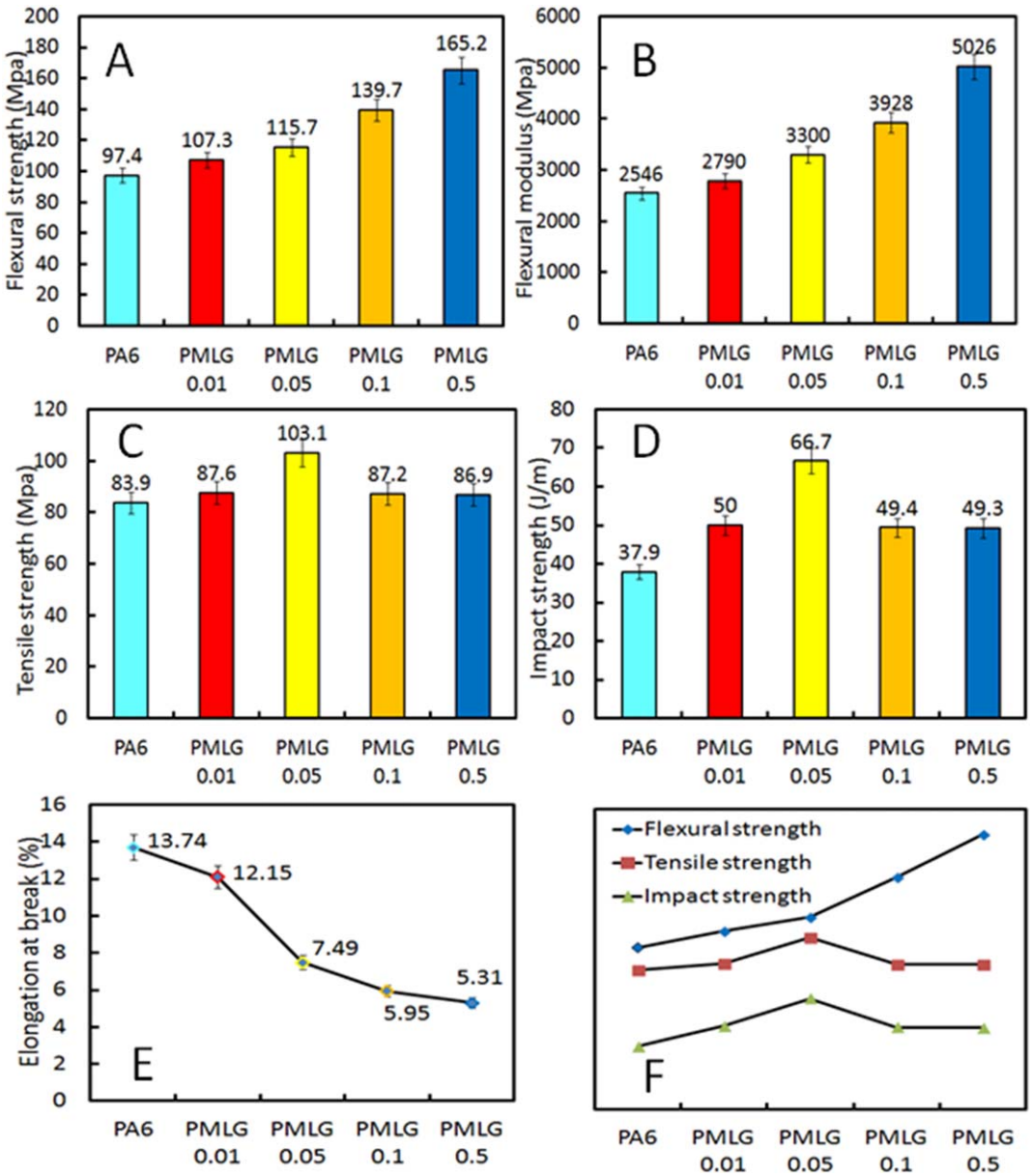

Figure 10. Mechanical properties testing: (A) flexural strength; (B) flexural modulus; (C) tensile strength; (D) impact strength; (E) elongation at break of PA6 and PMLG samples; (F) comparison on the changing trends of the strength. [Color figure can be viewed in the online issue, which is available at wileyonlinelibrary.com.]

Table VI. Mechanical Properties of Graphene/Polymer Nanocomposites

Polymer	Reinforcements	Graphene content (wt %)	Modulus increase (%)	Tensile strength increase (%)	References
PA6	TRGO	10	~47.2	_	53
PA11	FG	3	~25.8	~43.9	54
PA12	FG	3	~1.1	_	54
PBS	CRGO	2	~22	_	55
PVA	GO	2	~92.2	_	55
PA6	GO	1	~66.7	_	3
PA6	MLG	0.5	~97.4	~3.6	This work
PA6	MLG	0.05	~29.6	~22.9	This work

TRGO: thermally reduced graphene oxide; FG: functionalized graphene; CRGO: chemically reduced graphene oxide; GO: graphene oxide.

composite.)[46] It can be seen from Table V that the X_c of PMLG varies within a small range of 32.8–34.8% for the PMLG samples with 0.01–0.5 wt % MLG loading, which is also higher than that of pristine PA6 (31.8%), implying MLG can promote crystallization by acting as a nucleating agent too.[3] Moreover, the X_c of PMLG samples increased with increasing of MLG content below 0.1 wt % and decreased with the incorporation of more MLG sheets, indicating the excess MLG may block the mobility of PA6 chains and reduce the crystallization growth.[3] Furthermore, Figure 9(B) also shows the crystallization peaks become much more narrow relative to pristine PA6 with increasing MLG loading, which indicates that MLG can increase the crystallization speed of PA6 composites. The aforementioned results suggest that a small amount of MLG sheets has a significant influence on the crystallization aggregation or assembly behaviors of polymer chains. Therefore, DSC results prove the fact that MLG not only improves the crystallinity, but also increase the rate of crystallization of PA6.[49]

Mechanical Properties

Incorporating graphene into the polymer matrix can improve its mechanical properties.[50,51] It is found that the addition of MLG into the PA6 matrix has a significant positive influence on the mechanical behavior such as strength and modulus of PMLG samples. Figure 10(A,B) show the ultimate flexural strength and flexural modulus measurements for pristine PA6 and PMLG composites with different MLG contents. It is apparent that with an increase in MLG content, the flexural strength and flexural modulus of PMLG samples increases as well. Specifically, when the content of MLG is 0.5 wt %, the flexural modulus of PMLG samples (5026 MPa) is about 97% larger than that of pristine PA6 (2546 MPa), and the flexural strength of pristine PA6 is increased by 69% from 97.4 to 165.2 MPa.

Figure 10(C) compares the tensile strength of the pristine PA6 and PMLG samples. Unlike the flexural strength, the tensile strength of PMLG samples shows a trend of an initial increase and then a decrease. When incorporated with 0.05 wt % MLG, the tensile strength of PMLG (103.1 MPa) is improved by about 23% from 83.9 to 103.1 MPa. As the MLG content is further increased, the tensile strength falls to 87.2 MPa at 0.1 wt %. This phenomenon is because the MLG loading exceeds the critical level in which the excess MLG may form small agglomerates that play a role of stress concentration sites, thus becoming one of the possible reasons of the fracture of PMLG.[52] Moreover, the large number of oligomers in the samples may decrease the

Table VII. Preparation Process and Mechanical Properties of Graphene/Polymer Nanocomposites

Polymers	Reinforcements	Chemical reagents used	Time consuming (hours)	Modulus increase (%)	References
Epoxy	TRGO	H_2SO_4, HCL, HNO_3, $KCLO_3$	~116.5	~31	51
Epoxy	GO	KM_nO_4, MDI, DBDL, H_2SO_4, HNO_3, HCL	~92	~25	55
PVA	GO	H_2SO_4, HNO_3, HCL, formic acid, KM_nO_4, THF	~75	~52	55
PA6	FG	4-aminobenzoic, 6-aminocaproic acid, H_2SO_4, HCL, formic acid, KM_nO_4	~108	~290	57
PA6	TRGO	6-aminocaproic acid, H_2SO_4, KM_nO_4, H_2O_2	~237	~240	21
PA6	GO	MDI, DBDL, THF, H_2SO_4, HNO_3, HCL, formic acid, KM_nO_4	~38.5	~66.5	3
PA6	FG	H_2SO_4, KM_nO_4, HCL, 4-aminobenzoic, 6-aminocaproic acid, methanol	~259.5	~29	7
PA6	MLG	TDI, NaOH	~2	~97.4	This work

intermolecular interaction between polymers and lead to the reduction of the tensile strength. However, it is interesting that the flexural strength of PMLG samples does not decrease, which might be due to the content of MLG not reaching the critical level because of the loading mode of tensile test and flexural test is different. The impact strengths of pristine PA6 and PMLG samples are shown in Figure 10(D); the results are similar to that of the tensile strength. When the content of MLG is below 0.05 wt %, the impact strength increases with increase in MLG content, it is improved by about 76% from 37.9 to 66.7 J/m. After that, the impact strength of PMLG samples decreases from 66.7 to 49.4 J/m. It continues to decrease to 49.3 J/m when the content of MLG is 0.5 wt %.

According to earlier publications, graphene is very effective at enhancing the mechanical properties of polymer composites.[23] It is believed that the mechanical properties of graphene–polymer composites are determined by the degree of well dispersed graphene sheets and the strong interaction between graphene sheets and polymer matrix.[3] A good dispersion of graphene sheets in the polymer matrix was obtained by using modified graphene in earlier works. Even though the graphene used in this study was not modified, the reinforcement of PMLG nanocomposites is still efficient at loadings as low as 0.5 wt % MLG. Table VI lists the data of previous works in reference to the graphene reinforcement polymer. From the comparison between those works and our investigation, it is clearly that the graphene content of this work is relatively very low. There are probably three factors to achieve such results: (a) earlier works have indicated that it is not modified graphene, but unmodified graphene, that has obtained more remarkable enhancements especially in mechanical properties,[40] (b) it was demonstrated that multilayer graphene will give rise to higher levels of reinforcement than single-layer graphene with the optimum number of layers depending upon the separation of the graphene lakes in the polymer matrix[56] (c) the *in situ* polymerization method coupled with a good dispersion method (the ultrasonic cell crusher).

It can be seen clearly from Table VII that the modification process needed many chemical reagents and requires more time, which resulted in more pollution, more time consumption and higher costs in comparison with this work in which the effect of reinforcements was similar.

CONCLUSIONS

This work demonstrated an effective approach to prepare PA6/graphene nanocomposites by using unmodified multilayer graphene. The multilayer graphene sheets can be well dispersed in melted ε-caprolactam via an ultrasonic cell crusher at an optimal ultrasonic time and power. The thermal and mechanical properties of nanocomposites were investigated. TGA results indicate that nanocomposites demonstrated higher thermal stability than that of pristine PA6. The flexural strength, flexural modulus and impact strength were all drastically enhanced, while the formation of γ-crystalline was promoted. In addition, the crystallization temperature and crystallization velocity of nanocomposites were both improved. Moreover, relative to previous works that utilized modified graphene, this method was more suitable for commercial production while still capable of reaching similar or even improved properties of the composite. The improvement on the mechanical properties of PA6 matrix at low loading of MLG suggests the potential use of PA6/MLG nanocomposites in the fields of engineering plastics, mechanical, transportation, aerospace, medical, and electrical equipment, especially in automobile industry applications. For example, it can be used to fabricate the accessories for automobile manufacturing; such as exhaust gas filter, car frames for enhanced strength, wear resistant parts like bearing and so forth. Therefore, this method enabled the use of multilayer graphene with the application of industrial production implications.

ACKNOWLEDGMENTS

This study was supported by the National Natural Science Foundation of China (2013BAE02B03).

REFERENCES

1. Novoselov, K. S.; Falko, V. I.; Colombo, L.; Gellert, P. R.; Schwab, M. G.; Kim, K. A. *Nature* **2012**, *490*, 192.
2. Ferrari, A. C. *Solid State Commun.* **2007**, *143*, 47.
3. Zhang, X. Q.; Fan, X. Y.; Li, H. Z.; Yan, C. *J. Mater. Chem.* **2012**, *22*, 24081.
4. Novoselov, K. S.; Geim, A. K.; Morozow, S. V.; Jiang, D.; Zhang, Y.; Dubonos, S. V. *Science* **2004**, *306*, 666.
5. Potts, J. R.; Dreyer, D. R.; Bielawski, C. W.; Ruoff, R. S. *Polymer* **2011**, *52*, 5.
6. Sengupta, R.; Bhattacharya, M.; Bandyopadhyay, S.; Bhowmick, A. K. *Polym. Sci.* **2011**, *36*, 638.
7. Liu, H. H.; Hou, L. C.; Peng, W. W.; Zhang, Q.; Zhang, X. X. *J Mater. Sci.* **2012**, *47*, 8052.
8. Jin, J.; Rafiq, R.; Gill, Y. Q.; Song, M. *Eur. Polym. J.* **2013**, *49*, 2617.
9. Yoonessi, M.; Gaier, J. R. *ACS Nano* **2010**, *4*, 7211.
10. Cheng, S.; Chen, X.; Hsuan, Y. G.; Li, C. Y. *Macromolecules* **2012**, *45*, 993.
11. Kuila, T.; Bose, S.; Hong, C. E.; Uddin, M. E.; Khanra, P.; Kim, N. H. *Carbon* **2011**, *49*, 1033.
12. Teng, C. C.; Ma, C. C. M.; Lu, C. H.; Yang, S. Y.; Lee, S. H.; Hsiao, M. C. *Carbon* **2011**, *49*, 5107.
13. Yang, S. Y.; Lin, W. N.; Huang, Y. L.; Tien, H. W.; Wang, J. Y.; Ma, C. C. M. *Carbon* **2011**, *49*, 793.
14. Ramanathan, T.; Abdala, A. A.; Stankovich, S.; Dikin, D. A.; Herrera-Alonso, M.; Piner, R. D. *Nat. Nanotechnol.* **2008**, *l3*, 327.
15. Son, D. I.; Kim, T. W.; Shim, J. H.; Jung, J. H.; Lee, D. U.; Lee, J. M. *Nano Lett.* **2010**, *10*, 2441.
16. Song, P. G.; Cao, Z. H.; Cai, Y. Z.; Zhao, L. P.; Fang, Z. P.; Fu, S. Y. *Polymer* **2011**, *52*, 4001.
17. Shin, K. Y.; Hong, J. Y.; Lee, S.; Jang, J. *J. Mater. Chem.* **2012**, *22*, 7871.

18. Kim, H.; Abdala, A. A.; Macosko, C. W. *Macromolecules* **2010**, *43*, 6515.
19. Thanh, T. D.; Kapralkova, L.; Hromadkova, J.; Kelnar, I. *Eur. Polym. J.* **2014**, *50*, 39.
20. Li, J.; Tian, L.; Pan, N.; Pan, Z. *J. Polym. Eng. Sci.* **2014**, *54*, 1618.
21. Xu, Z.; Gao, C. *Macromolecules* **2010**, *43*, 6716.
22. Patole, A. S.; Patole, S. P.; Kang, H.; Yoo, J. B.; Kim, T. H.; Ahn, J. H. A. *J. Colloid. Interface Sci.* **2010**, *350*, 530.
23. Bao, C. L.; Guo, Y. Q.; Song, L.; Kan, Y. C.; Qian, X. D.; Hu, Y. *J. Mater. Chem.* **2011**, *21*, 13290.
24. Kim, H.; Kobayashi, S.; AbdurRahim, M. A.; Zhang, M. J.; Khusainova, A.; Hillmyer, M. A. *Polymer* **2011**, *52*, 1837.
25. Potts, J. R.; Lee, S. H.; Alam, T. M.; An, J.; Stoller, M. D.; Piner, R. D. *Carbon* **2011**, *49*, 2615.
26. Yun, Y. S.; Bae, Y. H.; Kim, D. H.; Lee, J. Y.; Chin, I. J.; Jin, H. *J. Carbon* **2011**, *49*, 3553.
27. Wicklein, B.; Kocjan, A.; Salazar-Alvarez, G.; Carosio, F.; Camino, G.; Antonietti, M. *Nat. Nanotechnol.* **2014**, *248*, 1.
28. Avila-Vega, Y. I.; Leyva-Porras, C. C.; Mireles, M.; Quevedo-Lopez, M.; Macossay, J.; Bonilla-Cruz, J. *Carbon* **2013**, *63*, 376.
29. Paci, J. T.; Belytschko, T.; Schatz, G. C. *J. Phys. Chem. C* **2007**, *111*, 18099.
30. Dikin, D. A.; Stankovich, S.; Zimney, E. J.; Piner, R. D.; Dommett, G. H.; Evmenenko, G. *Nature* **2007**, *448*, 457.
31. Morimune, S.; Kotera, M.; Nishino, T.; Goto, T. *Carbon* **2014**, *70*, 38.
32. Fu, Y. X.; Wang, X. M.; Mo, D. C.; Lu, S. S. *J. Mater. Sci.* **2014**, *49*, 2315.
33. Gayathri, S.; Jayabal, P.; Kottaisamy, M.; Ramakrishnan, V. *AIP Adv.* **2014**, *4*, 027116.
34. Cooper, A. J.; Wilson, N. R.; Kinloch, I. A.; Dryfe, R. A. W. *Carbon* **2014**, *66*, 340.
35. Hong, N. N.; Yang, W.; Bao, C. L.; Jiang, S. H.; Song, L.; Hu, Y. *Mater. Res. Bull.* **2012**, *47*, 4082.
36. Cai, D. Y.; Song, M. *J. Mater. Chem.* **2010**, *20*, 7906.
37. Chen, D.; Zhu, H.; Liu, T. X. *ACS Appl. Mater. Interface* **2010**, *2*, 3702.
38. Fouad, H.; Elleithy, R. *J. Mech. Behav. Biomed.* **2011**, *4*, 1376.
39. Liu, A. X.; Hong, Z. K.; Zhuang, X. L.; Chen, X. S.; Cui, Y.; Liu; Y. *Acta Biomater.* **2008**, *4*, 1005.
40. Bao, C. L.; Guo, Y. Q.; Song, L.; Hu, Y. *J. Mater. Chem.* **2011**, *21*, 13942.
41. Lv, R. T.; Cruz-Silva, E.; Terrones, M. *ACS Nano* **2014**, *8*, 4061.
42. Wang, Q.; Li, H.; Chen, L. Q.; Huang, X. J.; Zhong, D. Y.; Wang, E. G. *J. Electrochem. Soc.* **2003**, *150*, A1281.
43. Eswaraiah, V.; Balasubramaniam, K.; Ramaprabhu, S. *Nanoscale* **2012**, *4*, 1258.
44. Liu, Y.; Chen, Z. M.; Yang, G. S. *J. Mater. Sci.* **2011**, *46*, 882.
45. Zheng, D.; Tang, G. S.; Zhang, H. B.; Yu, Z. Z.; Yavari, F.; Koratkar, N. *Compos. Sci. Technol.* **2012**, *72*, 284.
46. Chatterjee, S.; Uesch, F.; Chu, B. T. T. *Nanotechnology* **2011**, *22*, 5714.
47. Bhattacharyya, A. R.; Potschke, P.; Haussler, L.; Fischer, D. *Macromol. Chem. Phys.* **2005**, *206*, 2084.
48. Liu, A. D.; Xie, T. X.; Yang, G. S. *Macromol. Chem. Phys.* **2006**, *207*, 701.
49. Bao, C. L.; Song, L.; Xing, W. Y.; Yuan, B. H.; Wilkie, C. A.; Huang, J. L. *J. Mater. Chem.* **2012**, *22*, 6088.
50. Wang, J. Y.; Yang, S. Y.; Huang, Y. L.; Tien, H. W.; Chin, W. K.; Ma, C. C. M. *J. Mater. Chem.* **2011**, *21*, 13569.
51. Rafiee, M. A.; Rafiee, J.; Wang, Z.; Song, H. H.; Yu, Z. Z.; Koratkar, N. *ACS Nano* **2009**, *3*, 3884.
52. Stankovich, S.; Dikin, D. A.; Dommett, G. H. B.; Kohlhaas, K. M.; Zimney, E. J.; Stach, E. A. *Nature (Lett)* **2006**, *442*, 282.
53. Steurer, P.; Wissert, R.; Thomann, R.; Mulhaupt, R. *Macromol. Rapid Commun.* **2009**, *30*, 316.
54. Jin, J.; Rafiq, R.; Gill, Y. Q.; Song, M. *Eur. Polym. J.* **2013**, *49*, 2617.
55. Verma, D.; Gope, P. C.; Shandilga, A.; Gupa, A. *Trans. Indian Inst. Met.* **2014**, *67*, 803.
56. Gong, L.; Young, R. J.; Kinloch, I. A.; Riaz, I.; Jalil, R.; Novoselov, K. S. *ACS Nano* **2012**, *6*, 2086.
57. Liu, H. H.; Peng, W. W.; Hou, L. C.; Wang, X. C.; Zhang, X. X. *Compos. Sci. Technol.* **2013**, *81*, 61.